Miscibility and Crystallization of Poly(β-hydroxybutyrate)/Poly(vinyl acetate-*co*-vinyl alcohol) Blends

Peixiang Xing,* Xin Ai, Lisong Dong, and Zhiliu Feng

Polymer Physics Laboratory, Changchun Institute of Applied Chemistry, Chinese Academy of Sciences, Changchun 130022, P. R. China

Received February 19, 1998; Revised Manuscript Received July 7, 1998

ABSTRACT: Poly(vinyl acetate-*co*-vinyl alcohol) copolymers (P(VAc-*co*-VA)) were synthesized by hydrolysis−alcoholysis of PVAc. The miscibility, crystallization, and morphology of poly(β-hydroxybutyrate) (PHB) and P(VAc-*co*-VA) blends were studied by differential scanning calorimetry, optical microscopy (OM), and SAXS. It is found that the P(VAc-*co*-VA)s with vinyl alcohol content of 9, 15, and 22 mol % will form a miscible phase with the amorphous part of PHB in the solution-cast samples. The melting-quenched samples of PHB/P(VAc-*co*-VA) blends with different vinyl alcohol content show different phase behavior. PHB and P(VAc-*co*-VA9) with low vinyl alcohol content (9% mol) will form a miscible blend in the melt state. PHB and P(VAc-*co*-VA15) with 15 mol % vinyl alcohol will not form miscible blends while PHB/P(VAc-*co*-VA15) blend with 20/80 composition will form a partially miscible blend in the melt state. PHB and P(VAc-*co*-VA22) with 22 mol % vinyl alcohol are not miscible in the whole composition range. The single glass transition temperature of the blends within the whole composition range suggests that PHB and P(VAc-*co*-VA9) are totally miscible in the melt. The crystallization kinetics was studied from the whole crystallization and spherulite growth for the miscible blends. The equilibrium melting point of PHB in the PHB/P(VAc-*co*-VA9) blends, which was obtained from DSC results using the Hoffman−Weeks equation, decreases with the increase in P(VAc-*co*-VA9) content. The negative value of the interaction parameter determined from the equilibrium melting point depression supports the miscibility between the components. The kinetics of spherulitic crystallization of PHB in the blends was analyzed according to nucleation theory in the temperature range studied in this work. The best fit of the data to the kinetic theory is obtained by employing WLF parameters and the equilibrium melting points obtained by DSC. The addition of P(VAc-*co*-VA) did not affect the crystalline structure of PHB, as shown by the WAXD results. The long periods of blends obtained from SAXS increase with the increase in P(VAc-*co*-VA) content. It indicates that the amorphous P(VAc-*co*-VA) was rejected to interlamellar phase corporating with the amorphous part of PHB.

Introduction

Bacterial-synthesized poly(β-hydroxybutyrate) is a crystalline polyester of great technological interest, because it is a truly biodegradable and highly biocompatible polymer.[1,2] This polyester has optical activity, piezoelectricity, and gas barrier properties. However, the stiffness and brittleness of PHB, due to its relatively high melting temperature and high crystallinity, have limited its application.

To overcome the shortcomings of PHB, and to obtain some useful new materials based on PHB, two approaches have been extensively studied. One approach is to biosynthesize copolyesters containing hydroxyalkanoate units other than 3HB units. For example, 3HB copolyesters containing 3-hydroxyvalerate,[3,4] 4-hydroxybutyrate,[5,6] and hydroxypropionate units[7] can be produced by *Alicaligenes eutrophus*. The composition of monomer units in these copolyesters can be controlled by using a mixture of different carbon sources in the culture medium. Depending on the chemical and compositional structures of these copolyesters, their physical properties, such as melting points and crystallinity, vary widely.

The second approach is to prepare miscible blends that consist of PHB and a flexible biodegradable polymer or plasticizer of lower molecular weight. It has been found that PHB is miscible with poly(ethylene oxide) (PEO),[8,9] synthesized atactic PHB,[10,11] poly(epichlorohydrin) (PECH),[12] poly(vinylidene fluoride) (PVDF),[13] poly(*p*-vinylphenol) (PVPh),[14−16] and poly(vinyl acetate) (PVAc),[17,18] respectively. However, PEO is biodegradable, but the other polymers are not biodegradable. Thus, PHB/PVAc and the other above-mentioned blends are partially biodegradable materials.

Many fundamental studies have been devoted to the melt miscibility of polymers. In this area, however, we still have a long way to go as far as the prediction of the miscibility behavior and structure−property relations of these polymer blends. The degree of miscibility of the components in a blend is of crucial importance with respect to its morphology and physical properties. A limited number of studies deal with the semicrystalline morphology of blends of crystallizable and amorphous polymers.

It is interesting to note that PHB and PVAc are isomers which were found to be miscible blends.[17,18] In this work, we try to change the molecular structure of PVAc via its hydrolysis−alcoholysis and introduction of the vinyl alcohol of random distribution into the PVAc backbone to study the relationship between miscibility and molecular structure.

Experimental Section

The poly(β-hydroxybutyrate) (PHB) was supplied by Aldrich, its melting temperature is 172 °C. The molecular weights of PHB and PVAc were determined by viscosity in chloroform,

* To whom correspondence should be addressed.

S0024-9297(98)00256-3 CCC: $15.00
Published on Web 09/15/1998

Table 1. Reaction Time, Degree of Hydrolysis, and Glass Transition Temperature for P(VAc-*co*-VA) Copolymers Used in This Work

polymer	reaction time (h)	degree of hydrolysis (mol %)	T_g (K)
PVAc			314
P(VAc-*co*-VA9)	8	9	317.4
P(VAc-*co*-VA15)	12	15	319.9
P(VAc-*co*-VA22)	19	22	321.5

they are M_n(PHB) = 2.93 × 10^5, M_n(PVAc) = 2.7 × 10^5, respectively. These polymers were not purified when they were used.

The blends of PHB and P(VAc-*co*-VA) were prepared by dissolving PHB and the copolymers in chloroform, the solutions were casted onto glass slides and then dried under vacuum at 70 °C for 48 h. The samples for wide-angle X-ray diffraction (WAXD) and small-angle X-ray scattering (SAXS) experiments were compression molded and isothermally crystallized at 95 °C for 24 h.

Synthesis of Poly(vinyl acetate-*co*-vinyl alcohol) Copolymers. Poly(vinyl acetate-*co*-vinyl alcohol) copolymers-(P(VAc-*co*-VA)) were obtained by hydrolysis−alcoholysis of PVAc at 50 °C in an acidic medium.[19,20] An 8 g sample of PVAc was dissolved in 1.5 dL of a stirred 9:1 (v/v) methanol−water mixture. Then, 2.5 mL of concentrated HCl was added to obtain an acid concentration of 0.2 M. The degree of hydrolysis was controlled by varying the time of reaction and was determined by titration of residual acetate groups. Reaction products with low degrees of hydrolysis were precipitated in water, followed by dissolution in methanol, and purified by Soxhlet extraction for about 4 h. For the synthesis method used, a random distribution of hydroxyl groups in the copolymer chain is expected.[21] Glass transition temperatures of the samples are in agreement with a random distribution of hydroxyl groups in the copolymer chain (see Table 1).

Experimental Conditions for Measurements. A Perkin-Elmer DSC-2C differential scanning calorimeter was employed to study the glass transition temperature (T_g), melting, and crystallization behavior of PHB, P(VAc-*co*-VA), and their blends (PHB/P(VAc-*co*-VA)). For T_g the samples were heated from 243 to 463 K (first scan) with a heating rate of 10 K/min and then maintained at 463 K for 2 min before rapid quenching to 243 K. The samples were then reheated to 463 K (second scan). The value of the midpoint of the transition was taken as the T_g.

To obtain the observed melting temperature (T_m') as a function of the crystallization temperature (T_c), the samples were melted at 463 K for 2 min, rapidly quenched to the desired T_c, isothermally crystallized until completely crystallized, and finally heated with a rate of 10 K/min in the DSC. The melting peak temperature was taken as the melting point (T_m').

The spherulitic growth rates were measured for PHB spherulites in the temperature range from 363 to 393 K for the blends with various P(VAc-*co*-VA9) contents (0, 20, 40, 60 wt %). At a given T_c, the spherulitic growth rate was obtained by photographing from time to time during the isothermal crystallization process under an optical microscope. The radius growth rate ($G = dr/dt$) was calculated from the slope of the lines connecting the radius r and its time on an r vs t plot. Thin films for polarized optical microscope observation were prepared by melting the casting films on a hot stage at 463 K for 2 min and then transferred as quickly as possible onto another hot stage at a prefixed T_c.

WAXD experiments were performed with a Philips PW1700 X-ray diffractometer using Cu Kα X-rays with a voltage of 30 kV and a current of 20 mA. SAXS measurements were performed using a compact Kratky system connected with the Philips PW1700 diffractometer. The incident beam slit was 80 μm and the receiving slit was 200 μm.

Results and Discussion

Miscibility and Phase Behavior of PHB/P(VAc-*co*-VA) Blends. Generally, thermal characterization of polymer blends is a well-known method for determining the miscibility of polymer blends. The miscibility between any two polymers in the amorphous state is detected by the presence of a single glass transition temperature (T_g) intermediate between those of the two component polymers.[22] So it is important to establish the T_g behavior of PHB/P(VAc-*co*-VA) blends. The blends of PHB and P(VAc-*co*-VA) with three different vinyl alcohol contents (9, 15, 22 mol %) were studied.

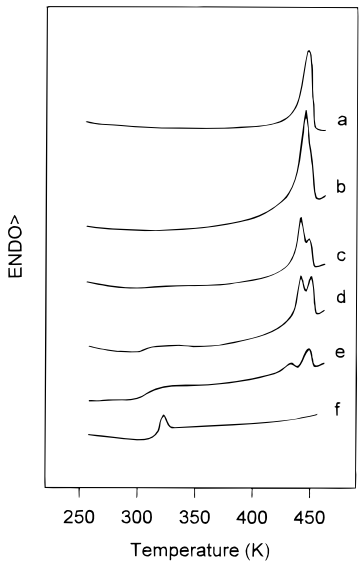

Figure 1. DSC curves of solution-blended PHB/P(VAc-*co*-VA9) blends: (a) 100/0, (b) 80/20, (c) 60/40, (d) 40/60, (e) 20/80, (f) 0/100.

The results show that at the first heating scan no obvious glass transition was observed for the cast PHB/P(VAc-*co*-VA9) (80/20) due to the high crystallinity of PHB in the blends. Only a single glass transition was observed in the 60/40, 40/60, and 20/80 wt % PHB/P(VAc-*co*-VA9) blends, respectively (Figure 1). The T_gs of the blends are higher than 290 K and are between the T_gs of the two components, which indicates that the amorphous phases of the casting films of PHB/P(VAc-*co*-VA9) blends are miscible. Similarly, the blends of PHB/P(VAc-*co*-VA15) and PHB/P(VAc-*co*-VA22) also show single glass transition, which are between the T_gs of the two components, in samples with compositions of 60/40, 40/60, and 20/80, respectively, while no obvious glass transition was observed in the sample with composition 80/20, due to its high crystallinity. This also indicates that the amorphous phases of the casting films of this blend system are miscible.

It is reported that the blends of PHB and poly(vinyl alcohol) (PVA),[23] prepared by solution casting, are partially miscible in the amorphous phase by solid-state high-resolution ^{13}C NMR and density measurement. So, we may consider that copolymer P(VAc-*co*-VA) is a random composition of monomers of PVAc and PVA. So the miscibility existing in the amorphous part of PHB/P(VAc-*co*-VA) is in agreement with the results of PHB/PVAc[17,18] and PHB/PVA[23] blends.

After the first heating to 190 °C, the samples were quenched to −30 °C gain heated to 190 °C for a second scan. However, during the second scan, the three blend systems showed different thermal behavior. For the PHB/P(VAc-*co*-VA9) blends, a single glass transition was observed (Figure 2). The T_g values of the blends varied with the compositions of the blends. This means

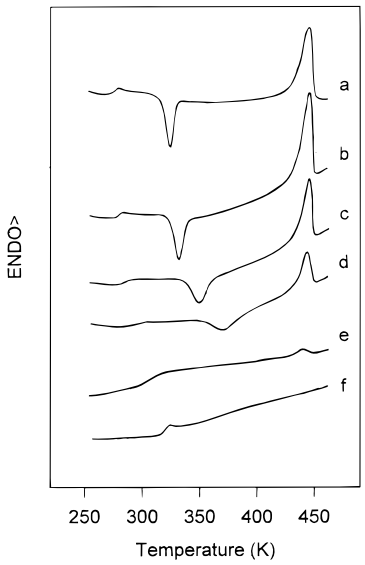

Figure 2. DSC curves of melt quenched PHB/P(VAc-*co*-VA9) blends: (a) 100/0, (b) 80/20, (c) 60/40, (d) 40/60, (e) 20/80, (f) 0/100.

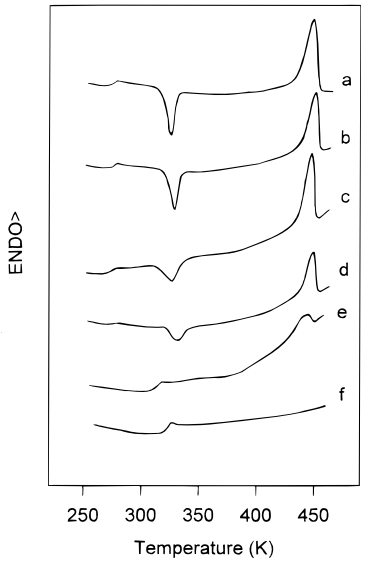

Figure 3. DSC curves of melt quenched PHB/P(VAc-*co*-VA15) blends: (a) 100/0, (b) 80/20, (c) 60/40, (d) 40/60, (e) 20/80, (f) 0/100.

Table 2. Glass Transition Temperatures (T_gs) of Pure PHB, P(VAc-*co*-VA9), and PHB/P(VAc-*co*-VA9) Blends Obtained by DSC

PHB/P(VAc-*co*-VA9)	T_g (K)	PHB/P(VAc-*co*-VA9)	T_g (K)
100/0	276.5	40/60	294.1
80/20	280.2	20/80	302.6
60/40	285.4	0/100	317.4

that these blends are miscible in the melt state (Figure 2, Table 2).

On the contrary, the PHB/P(VAc-*co*-VA15) blends 80/20, 60/40 and 40/60 each show one T_g, which is equal to the T_g of pure PHB (Figure 3), which means that they are immiscible in the melt state. For the blend PHB/P(VAc-*co*-VA15) 20/80, only one T_g (curve e in Figure 3) is found, showing some degree of inward shift comparing with the T_g of P(VAc-*co*-VA15), which indicates that this blend at composition 20/80 is partially miscible in the melt state. For the PHB/P(VAc-*co*-VA22) 80/20, 60/40, and 40/60 blends, also only one T_g value

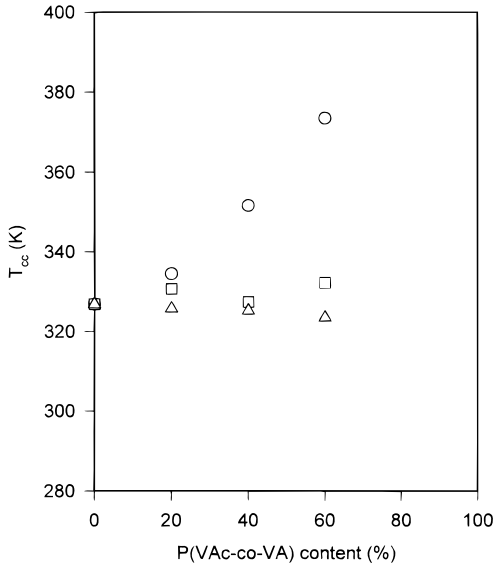

Figure 4. The temperature of the cold crystallization peak of PHB/P(VAc-*co*-VA) blends versus composition: (○) PHB/P(VAc-*co*-VA9) blends, (□) PHB/P(VAc-*co*-VA15) blends, (△) PHB/P(VAc-*co*-VA22) blends.

was observed, which is also equal to the T_g of PHB. The PHB/P(VAc-*co*-VA22) (at composition 20/80) shows two T_gs, which are equal to those of the two pure polymers, respectively. These clearly indicate that the PHB/P(VAc-*co*-VA22) blend is immiscible in the melt state. Because the T_gs of P(VAc-*co*-VA15) and P(VAc-*co*-VA22) are in the temperature range of the cold crystallization peak of pure PHB, it is hard to observe the T_gs of copolymer in the immiscible blends (high PHB content).

In addition to the T_g method, the cold crystallization temperature and melting point in the heating scan of quenched blends (at second heating run) can be used together to identify the miscibility of the three blend systems. Generally, cold crystallization takes place at a temperature above the T_g of the blends where the crystallizable polymer chains possess enough segmental mobility to crystallize. For the blends of PHB/P(VAc-*co*-VA9) 80/20, 60/40, and 40/60, the cold crystallization peaks move toward higher temperatures with the increase in P(VAc-*co*-VA9) content (Figures 2 and 4). The increase in the cold crystallization peak temperature observed may be explained by considering that the crystallization process takes place from a single homogeneous phase, and the T_g increases with P(VAc-*co*-VA9) content because the T_g of P(VAc-*co*-VA9) is higher than the T_g of PHB. This means these blends are miscible. When P(VAc-*co*-VA9) reaches 80%, cold crystallization does not show up on the DSC scan, which may be due to the high T_g of this blend or because the enthalpy is too small to be measurable.

In contrast, the blends of PHB/P(VAc-*co*-VA15) behave differently: for all the blends the temperatures of the cold crystallization peaks are almost unchanged and are approximately the same as the temperature of cold crystallization peak of pure PHB (Figures 3 and 4). Hence, the cold crystallization of PHB in the blends is not affected by the amorphous P(VAc-*co*-VA15), which indicates that the blends 80/20, 60/40, and 40/60 are immiscible. Similarly, the cold crystallization peak temperatures of PHB/P(VAc-*co*-VA22) blends 80/20, 60/40, and 40/60 (Figure 4) are almost unchanged, which also indicates that these blends of PHB/P(VAc-*co*-VA22) are immiscible in the melt state.

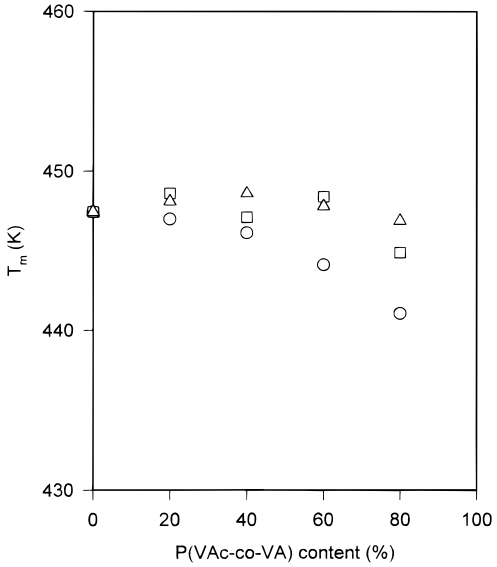

Figure 5. The melting temperature of PHB/P(VAc-*co*-VA) blends at the second heating scan: (○) PHB/P(VAc-*co*-VA9) blends, (□) PHB/P(VAc-*co*-VA15) blends (△) PHB/P(VAc-*co*-VA22) blends.

In another aspect, the melting behavior of the crystallizable component is affected by the amorphous component in the miscible blends, while the melting behavior will not be affected by the second amorphous component in immiscible blends. For the PHB/P(VAc-*co*-VA9) blends, the melting temperatures of PHB in the blends decrease with the increase in P(VAc-*co*-VA9) content (Figures 2 and 5), which indicates that the blends are miscible. For PHB/P(VAc-*co*-VA15) blends, the melting temperatures of PHB in the blends 80/20, 60/40, and 40/60 (Figures 3 and 5) are almost the same as that of pure PHB, which indicates that the blends 80/20, 60/40, and 40/60 are immiscible. Only a decrease of the melting temperature was observed in a blend of PHB/P(VAc-*co*-VA15) 20/80. Combined with the T_g shifts, this means that some degree of miscibility exists in this blend. So it may be considered that the blend of this composition is partial miscible. Similarly, the melting temperature of quenched PHB/P(VAc-*co*-VA22) blends (Figure 5) are almost the same, which means that they are immiscible in the melt state.

So PHB/P(VAc-*co*-VA9) blends are miscible in the melt in the whole composition range, whereas PHB/P(VAc-*co*-VA15) blends are immiscible (phase separate) in the melt state with the exception of the 20/80 blend (which shows some miscibility). Likewise, the blends of PHB/P(VAc-*co*-VA22) are also immiscible (phase separate) in the melt state in the whole composition range. In other words, blends of PHB/P(VAc-*co*-VA15) and PHB/P(VAc-*co*-VA22) possess low critical solution temperature (LCST). The phase diagrams of blends of PHB and P(VAc-*co*-VA) with different vinyl alcohol contents are shown in Figure 6.

Glass Transition Temperatures of Miscible PHB/P(VAc-*co*-VA9) Blends. The values of T_gs of PHB/P(VAc-*co*-VA9) blends during the second heating scan, when the samples were rapidly quenched from the melt state, are listed in Table 2. Pure PHB showed a T_g of 276.5 K, which is close to the values (277−282 K) given in the literature.[12,17,24,25] The small difference between these values could be attributed to the different molecular weights. The T_g value obtianed for P(VAc-*co*-VA9) is 317.4 K.

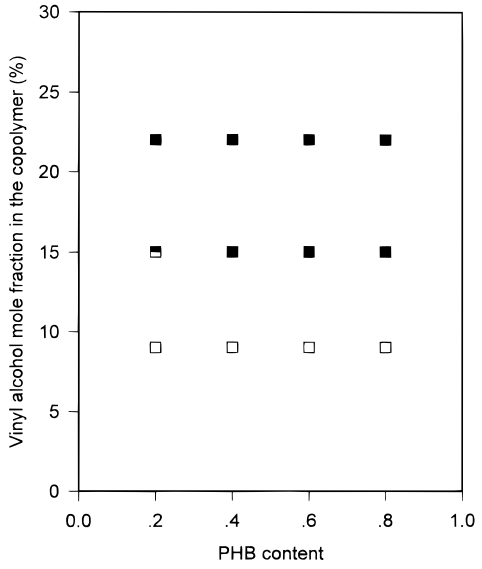

Figure 6. Phase diagram of PHB and P(VAc-*co*-VA) with different vinyl alcohol content: (□) miscible, (⬒) partial miscible, (■) immiscible

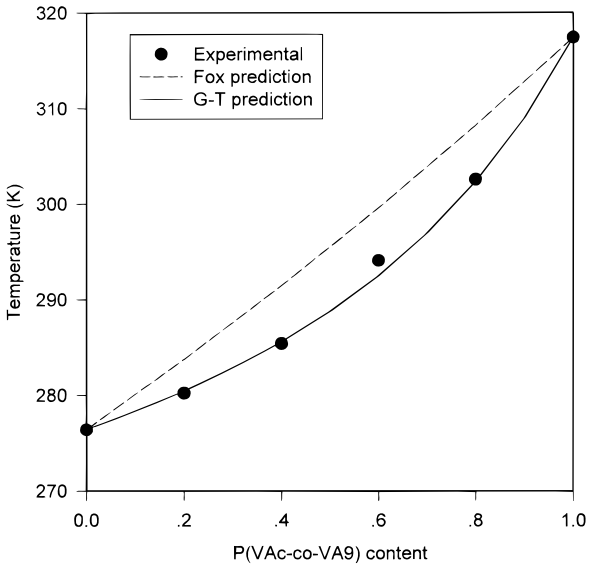

Figure 7. The glass transition behavior of PHB/P(VAc-*co*-VA9) blends: (●) experimental points, (- -) the Fox equation, (−) the Gordon−Taylor equation.

The dependence of T_g on the composition of the miscible PHB/P(VAc-*co*-VA9) blends is illustrated in Figure 7. For polymer blends their T_g can be predicted by several equations, such as the Fox equation,[26] Gordon−Taylor equation,[27] Couchman−Karasz equation,[28] Kwei equation.[29] The most commonly employed equation is the Gordon−Taylor expression (eq 1)[27] with the K parameter treated as an arbitrary fitting parameter:

$$T_g = \frac{W_1 T_{g1} + W_2 T_{g2}}{W_1 + K W_2} \qquad (1)$$

W_1 and W_2 are the weight fractions of components 1 and 2, respectively (in the amorphous phase); T_{g1} and T_{g2} are the respective T_gs of the pure components. The K parameter is often related to the strength of intermolecular interactions between the blend components.[27] Positive deviations of linear behavior ($K = 1$) with the

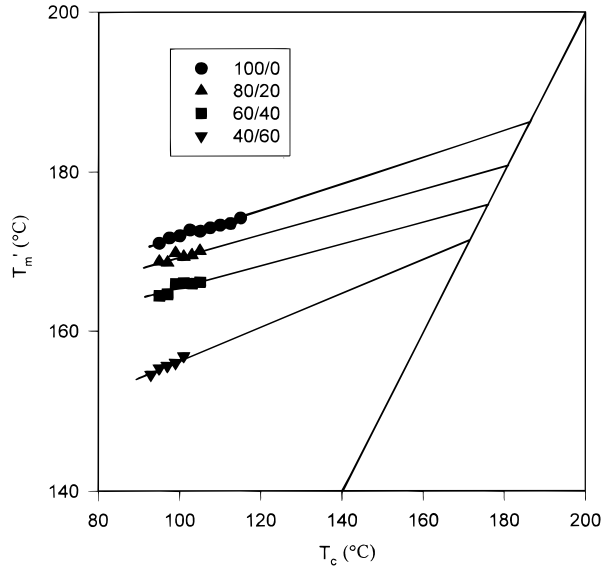

Figure 8. Hoffman−Weeks plots for PHB/P(VAc-*co*-VA9) blends employing data from DSC.

resultant high K values are expected for blends with restricted chain mobility. The predicted curves produced with the Fox and Gordon−Taylor equations are shown in Figure 7 (curves a and b) using T_g(PHB) = 276.5 K and T_g(P(VAc-*co*-VA9)) = 317.4 K. From Figure 7, it is seen that the glass transition behavior of these blends cannot be predicted by the Fox equation, but they fit the Gordon−Taylor equation very well when the K value of 0.43 was used. The small K value (<1) also means that there is no strong interaction between the two components.

Equilibrium Melting Temperature and Interaction Parameters. The miscibility of polymer blends with one semicrystalline component can be determined by melting point depression. Thermodynamic considerations predict that the chemical potential of a polymer will be decreased by the addition of a miscible diluent. If one polymer is crystallizable, its decrease in chemical potential will result in a decreased equilibrium melting point. The extent of the melting point depression in such systems will provide a measure of the interaction parameter, which is described by the Flory−Huggins theory.[30,31]

The Hoffman−Weeks equation[32] was used to derived the equilibrium melting temperature from the relation between the observed melting point T_m' and the isothermal crystallization temperature T_c, which is a very convenient method:

$$T_m' = \frac{T_c}{\gamma} + \left(1 - \frac{1}{\gamma}\right) T_m^\circ \qquad (2)$$

where γ is the ratio of the initial to the final lamellar thickness and T_m° is the equilibrium melting point. T_m° is obtained from a plot of T_m' as a function of T_c by extrapolating the linear data until it intersects with the line of $T_m' = T_c$.

The melting points T_m' with different T_c for pure PHB and for PHB crystallized in the blend were studied by DSC (Figure 8). The equilibrium melting point T_m° obtained from eq 2 is often related to the different thermal treatments employed in the experiments such as crystallization temperature range, time of crystallization, and scanning rate. Under the conditions described in the Experimental Section, Figure 8 gives the best-fit T_m' versus T_c lines obtained for PHB/P(VAc-*co*-VA9) blends. So the equilibrium melting point of the polymer blends of PHB/P(VAc-*co*-VA9) were obtained. The values of T_m° for blends determined by this method are listed in Table 3. In this system we found that the equilibrium melting point of pure PHB is lower than that reported in some other works.[8,25,33] Perhaps it is due to the molecular weight difference. It is clearly seen that the equilibrium melting point shows a decrease with the increase in the amorphous component P(VAc-*co*-VA9). The fact that the melting point depression is well observed in the PHB/P(VAc-*co*-VA9) blends means that the PHB/P(VAc-*co*-VA9) blends are miscible.

Table 3. Equilibrium Melting Temperature (T_m°) for Pure PHB and PHB/P(VAc-*co*-VA9) Blends

PHB/P(VAc-*co*-VA9)	T_m° (°C)	PHB/P(VAc-*co*-VA9)	T_m° (°C)
100/0	186.0	60/40	176.0
80/20	180.5	40/60	171.0

In polymer−polymer blends, miscibility is controlled by a thermodynamic process. The Flory−Huggins interaction parameter, χ_{12}, plays a decisive role in the melting behavior of crystalline polymer−amorphous polymer systems. Upon blending a crystallizable PHB with amorphous P(VAc-*co*-VA9), a depression in the equilibrium melting temperature of the crystallizable PHB is observed. So, the melting temperature depression method is employed to measure the interaction parameter χ_{12} in this work. We may use the Flory−Huggins equation[30] to get the Flory−Huggins interaction parameter χ_{12}

$$\frac{1}{T_m^{\circ\prime}} - \frac{1}{T_m^\circ} = -\frac{RV_{2u}}{\Delta H_f}\left(\frac{\ln \phi_2}{m_1} + \left(\frac{1}{m_1} - \frac{1}{m_2}\right)\phi_1\right) - \frac{RV_{2u}}{\Delta H_f V_{1u}} \chi_{12} \phi_1^{\,2} \qquad (3)$$

where $T_m^{\circ\prime}$ and T_m° are the equilibrium melting points of the blend and homopolymer, respectively, ΔH_f is the heat of fusion for the 100% crystallizable component, V_{1u} and V_{2u} are the molar volumes of the repeat units of the noncrystallizable and crystallizable component, and m_1, ϕ_1 and m_2, ϕ_2 are the degrees of polymerization and the volume fractions of noncrystallizable polymers 1 and crystallizable polymer 2, respectively. χ_{12} is the Flory−Huggins interaction parameter. Equation 3 may be applied to PHB/P(VAc-*co*-VA9) blends.

In this study, because the molecular weights of P(VAc-*co*-VA9) and PHB are high enough, approximately equal, and inversely proportional to the degree of polymerization, the terms m_1 and m_2 in eq 3 vanish. Taking into account these considerations, eq 3 can be expressed as

$$\frac{1}{T_m^{\circ\prime}} - \frac{1}{T_m^\circ} = -\frac{RV_{2u}}{\Delta H_f} \chi_{12} \phi_1^{\,2} \qquad (4)$$

from which χ_{12} can be directly evaluated by plotting ΔT_m° vs ϕ_1^2.

In eq 4, if χ_{12} is assumed to be independent of composition, a plot of the left-hand side versus ϕ_1^2 should give a straight line passing through the origin. To calculate the left-hand side of eq 4, the parameter values used are as follows: V_{1u} (= 69 cm^3)[34] is the repeat unit molar volume of P(VAc-*co*-VA9), V_{2u} (= 75 cm^3)[8] is

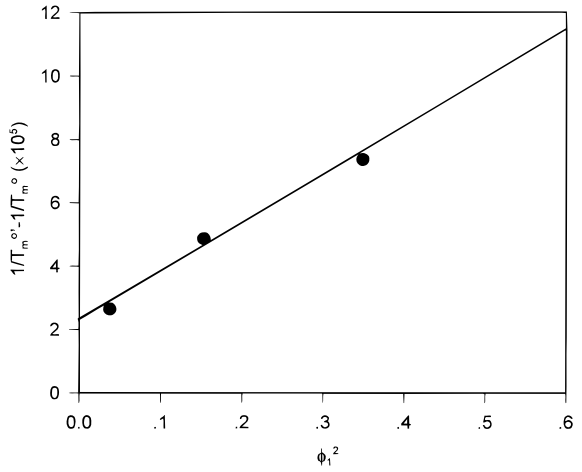

Figure 9. Application of the Flory−Huggins equation for PHB/P(VAc-*co*-VA9) blends

the repeat molar volume of PHB, and ΔH_f (3001 cal)[8] is the enthalpy of fusion for completely crystalline PHB. In Figure 9, The line passing through the experimental points intercepts the axis at 0.021 and has a slope of 1.5×10^{-4}. The fact that this line does not pass through the origin is usually attributed to a residual entropic effect that is neglected in the derivation of the equation or attributed to a possible composition dependence of χ_{12}. Such results were already reported by Paul et al.[35−37] In PHB/P(VAc-*co*-VA9) blend systems, we approximately treat the slope of the line in Figure 9 as $RV_{2u}\chi_{12}/\Delta H_f$ due to the very small positive intercept (0.021). The Flory−Huggins interaction parameter thus obtained is −0.21, which is close to the value of −0.073 for PHB/PVAc blends reported by Martuscelli.[17] The negative value of χ_{12} clearly indicates that the polymer pairs of PHB and P(VAc-*co*-VA9) will form miscible blends in the melt state.

Spherulitic Growth Kinetic. There are many works studying the crystallization kinetics in homopolymers via determining spherulitic growth rates.[37−40] The method often used to deal with the experimental results was established by Hoffman, Lauritzen, and co-workers,[41−43] and is called the Lauritzen−Hoffman theory. The Lauritzen−Hoffman theory has been extended to study the crystallization kinetics in miscible semicrystallizable/amorphous polymer blends.[30,44−46] In this work, the spherulite growth rates of pure PHB and PHB/P(VAc-*co*-VA9) blends were determined by observation with a polarizing optical microscope. Thin films of PHB/P(VAc-*co*-VA9) blends isothermally crystallized in the temperature range 363−393 K showed a spherulitic morphology for all compositions examined. The spherulite growth rate, G, was constant until impingement took place. In blends, the rate of spherulite growth at a given temperature is primarily governed by the composition of the melt at the growing lamellar front, and a steady-state growth indicates constancy of the melt composition. The linear dependence shown in Figure 10 is representative of all blends investigated which were crystallized at 90 °C. This indicates that, in the range of T_cs explored, while the growing PHB phase extracts pure PHB from the mixed melt, the rejected P(VAc-*co*-VA9) does not migrate toward the molten mixed phase. The P(VAc-*co*-VA9) remains trapped in the immediate vicinity of the growing PHB crystals, in the space either between the lamellae

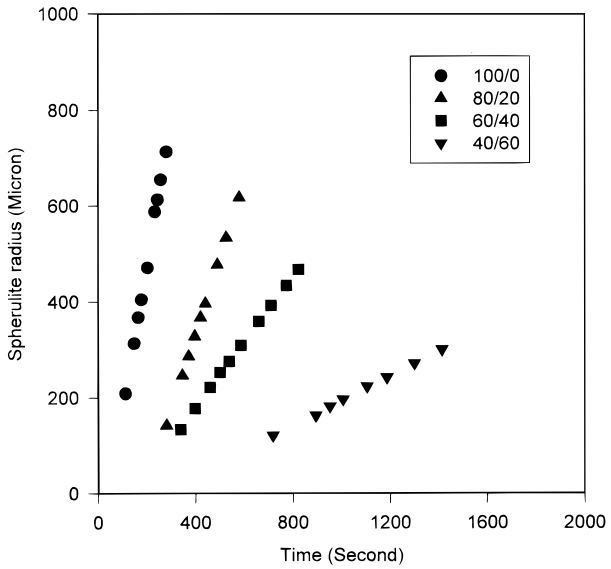

Figure 10. Spherulite radius as a function of time for the PHB/P(VAc-*co*-VA9) blends isothermally crystallized at 90 °C.

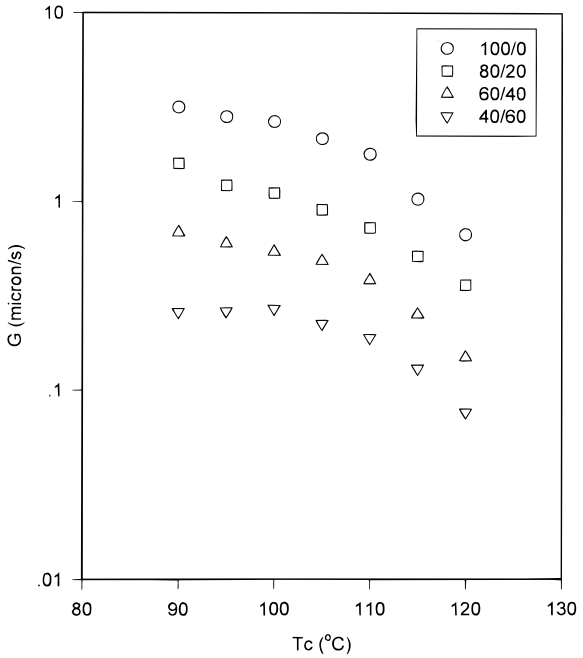

Figure 11. Radial growth rate (G) as a function of T_c for PHB/P(VAc-*co*-VA9) blends.

(interlamellarly) or between bundles of lamellae (interfibrillarly), leaving the melt composition unchanged.

It is also clearly seen from Figure 10 that the slope of the lines change to lower values upon increasing the P(VAc-*co*-VA9) content. The dependence of G on T_c for PHB and PHB/P(VAc-*co*-VA9) blends is shown in Figure 11, from which it can be seen that for PHB/P(VAc-*co*-VA9) blends the rate of spherulite growth at a given T_c decreases with the increase in P(VAc-*co*-VA9) content. The presence of the amorphous P(VAc-*co*-VA9) with high T_g in the blends remarkably decreases the rate of PHB crystallization. Generally, there are three main factors that can be taken into account to explain the crystallization rate depression in the miscible semicrystalline/amorphous polymer with high T_g: (a) a decrease of segmental mobility of the semicrystalline polymer molecules, transporting across the liquid−solid interface, due to the high T_g of the blends; (b) a dilution effect

that reduces the number of crystallizable segments on the front of the growing spherulite; (c) a decrease in undercooling due to the melting point depression. A crystallization rate depression of a magnitude similar to the ones shown in Figure 11 has been reported for miscible blends of PVDF/PMMA.[30] In the PVDF/PMMA system the growth rate decrease was mainly attributed to the changes in fluidity of the melt caused by the higher T_g of the blends than the pure PVDF. Similarly, the same reason may be used to explain the growth rate depression in the PHB/P(VAc-*co*-VA9) system.

The Lauritzen−Hoffmann model,[42] as described below, was used to analyze the spherulite crystallization behavior of homopolymer and some semicrystalline/amorphous polymer blends.[25,44−46] And many good results were obtained, such as for PVDF/PMMA.[45] This theory is also used to analyze the spherulite crystallization behavior of PHB/P(VAc-*co*-VA9) blends in this work. The equation is

$$G = G_0 \exp\left[\frac{-U^*}{R(T - T_\infty)}\right] \exp\left(\frac{-K_g}{fT\Delta T}\right) \qquad (5)$$

where the preexponential factor G_o contains terms which are essentially temperature-independent. U^* is the activation energy for transportation of crystallizable segments to the crystallization front. T_∞ is the temperature below which such motion ceases. T is the crystallization temperature. $\Delta T = T_m - T$ and is the degree of undercooling. T_m is the equilibrium melting point. f is a factor which accounts for the variation in the enthalpy of fusion ΔH_f with temperature and is given by $f = 2T/(T_m + T)$. K_g is the nucleation constant and it can be expressed as[42,43]

$$K_g = \frac{nb_o\sigma\sigma_e T_m}{\Delta H_f k} \qquad (6)$$

where σ and σ_e are the lateral and end surface free energies, respectively, of the growing crystal, b_o is the molecular thickness, and k is the Boltzmann constant. The value of n depends on the regime of crystallization.

It is important to note that the parameters U^* and T_∞ (eq 5) were treated as variables in order to maximize the quality of the fit to eq 5. In many cases in the literature these parameters have simply been assigned the "universal" values[42] $U^* = 1500$ cal mol^{-1} and $T_\infty = T_g - 30$ K, as appropriate to many polymers, or the Williams−Landel−Ferry (WLF)[47] values $U^* = 4120$ cal mol^{-1} and $T_\infty = T_g - 51.6$ K. It is often most convenient to rearrange eq 5 as follows

$$\ln G + \frac{U^*}{R(T - T_\infty)} = \ln G_0 - \frac{K_g}{T(\Delta T)f} \qquad (7)$$

and view the growth rate data in the form of a plot of the left-hand side of eq 7 vs $1/[T_\infty(\Delta T)f]$, where the slope is $-K_g$. The K_g obtained with the above analysis from Figure 12 is 4.61×10^5 (K^2) for pure PHB, which is close to the results reported in the literature by Martuscelli.[17] Besides, some results have already been obtained for pure PHB[25] and blends containing PHB.[25] It is found that the regime transition from regime II to regime III exists in the crystallization process of PHB and atactic PHB blends at about 120−140 °C. So in our analysis the regime is assigned to be regime III, and $n = 4$ is adopted. The derived K_gs can be used to calculate σ_e

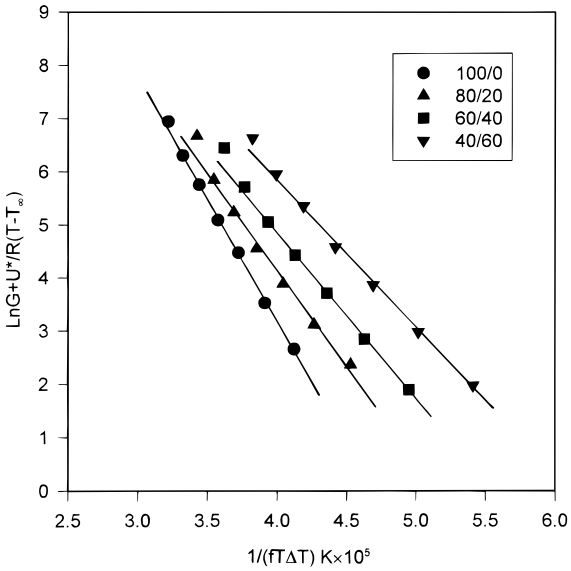

Figure 12. Kinetic analysis of crystallization rate constant data employing WLF constants and equilibrium melting temperatures.

Table 4. Values of K_g and σ_e for Pure PHB and PHB/PVPh Blends

PHB/PVPh	K_g(III) (K^2)	σ_e (erg cm^{-2})
100/0	4.61×10^5	42.74
80/20	3.78×10^5	35.05
60/40	3.21×10^5	29.76
40/60	2.80×10^5	25.96

Table 5. Crystallinity of PHB/P(VAc-*co*-VA9) Blends Isothermally Crystallized at 95 °C

PHB/P(VAc-*co*-VA9)	$X_{c,x}$	X_c(PHB)
100/0	0.598	0.598
80/20	0.463	0.579
60/40	0.368	0.614

(and the work of chain folding (q)) for PHB, using the empirical relation[48]

$$\sigma = \alpha(\Delta H_f)(a_0 b_0)^{1/2} \qquad (8)$$

with $\alpha = 0.25$ appropriate for high-melting polyesters (e.g., poly(phenylene sulfide)[49] and poly(pivalolactone)[40]) and the use of literature values of $a_o = 6.6$ Å, $b_o = 5.8$ Å[33], and $\Delta H_f = 1.85 \times 10^8$ J m^{-3}, eq 8 yields $\sigma = 29$ erg cm^{-2} and $\sigma_e = 42.74$ erg cm^{-2} (Table 4). The latter value agrees well with a previously reported value of 38 ± 6 erg cm^{-2} determined by measurements of lamellar thickness.[33] These values are different from the values (96 erg cm^{-2}) reported for PHB and poly(epichlorohydrin) (PECH).[12] The reason for the difference, pointed out by Marchessault,[50] was the value of α. The changes of the values of K_g(III) and σ_e with blend composition are listed in Table 4. Both values decrease with the increase in P(VAc-*co*-VA9) content, which indicates that the crystallization ability of PHB decreases with increasing P(VAc-*co*-VA9) content in blends.

The work of chain folding, q ($q = 2a_o b_o \sigma_e$), has been found to be one parameter most closely correlated with molecular structure.[42] Some work[40,42] has reported that q is roughly proportional to chain stiffness. Polyethylene and PCL with moderately stiff chains without side group have $q \sim 5$ kcal mol^{-1}.[51,52] The value $q = 4.4$ kcal mol^{-1} obtained for pure PHB fits into the category of moderately stiff chains. This value is less than 7.9 kcal

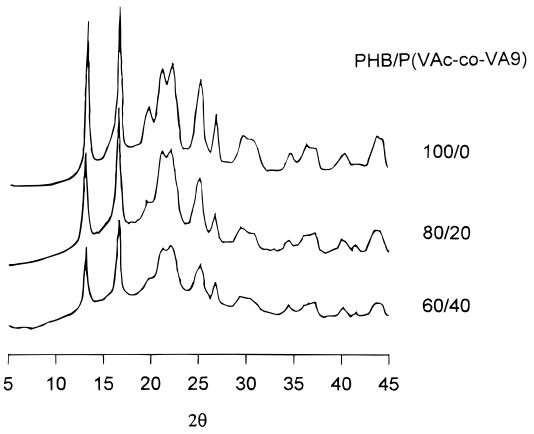

Figure 13. WAXD profiles of isothermally crystallized (at 95 °C) PHB/P(VAc-*co*-VA9) blends.

mol^{-1} for poly(pivalolactone),[53] which has two methyl side groups compared to one methyl for PHB.

Morphology

It is possible to use a wide spectrum of morphologies to study semicrystalline/amorphous polymer blends. And a proper evaluation of the properties of the blends requires a further understanding of the different structures. Studies on the structure of the crystallized PHB in its blends with PMMA and PECH were carried out with WAXD and SAXS.[54,55] The X-ray diffraction results of PHB/P(VAc-*co*-VA9) blends are shown in Figure 13. Comparing the spectrum of the pure PHB with that of the blends, it is seen that the *d* spacing values are constant for the (1 1 0), (0 0 2), and (0 2 0) crystallographic planes, which indicates that the PHB unit cell is not changed in the blends. Meanwhile, the results of simulations also show that the unit cell parameters are the same in both pure PHB and PHB in blends. By comparison with pure PHB, the intensities of the crystalline peaks of PHB/P(VAc-*co*-VA9) 80/20 and 60/40 decrease obviously, which implies that the addition of P(VAc-*co*-VA9) will hinder the crystallization of PHB in the blend.

The crystallinity $X_{c,x}$ of the blends and crystallinity of PHB components X_c(PHB) were also obtained from WAXD. The crystallinity of the blends decreases with the increase in P(VAc-*co*-VA9) content, while the crystallinity of the PHB component X_c(PHB) is similar to that of pure PHB.

The lamellar periodicities of PHB were determined by analysis of the small-angle X-ray scattering (SAXS) patterns of PHB/P(VAc-*co*-VA9) blends. The desmeared SAXS profiles of the isothermally crystallized pure PHB and PHB/P(VAc-*co*-VA9) blends (Figure 14) show the presence of a maximum, which is associated with the long period between the centers of adjacent lamellae. The curves are plotted as I^2q vs θ. This reflects the so-called "Lorentz" correction, which accounts for the isotropic nature of the lamellar system. The scattering vector magnitude is defined by $q = 4\pi \sin \theta/\lambda$, where θ is half of the scattering angle and λ is the wavelength of the radiation. The lamellar periodicity (L) can be determined by[56]

$$L = \frac{2\pi}{q_{max}} \tag{9}$$

where q_{max} is the q value at a maximum SAXS intensity.

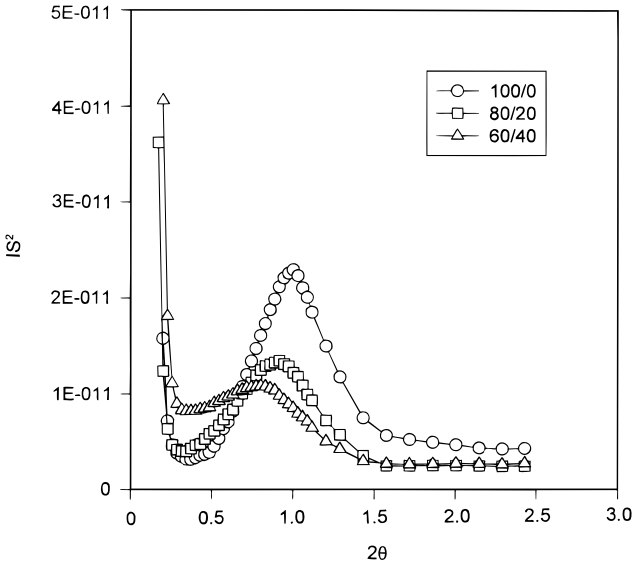

Figure 14. Desmeared SAXS profiles of isothermally crystallized (at 95 °C) PHB/P(VAc-*co*-VA9) blends.

Table 6. Long Period Values (Å) for Isothermally Crystallized (at 95 °C) Pure PHB and PHB/P(VAc-*co*-VA9) Blends

PHB/P(VAc-*co*-VA9)	long period (Å)
100/0	88.0
80/20	96.3
60/40	110.0

L of the pure PHB is 8.8 nm in this study. The magnitude of this long period is in the range of those found by Doi et al.[11] for PHB. It is observed that the long period increases with the increase in amorphous P(VAc-*co*-VA9) content (Table 6). This kind of increase in the lamellar periodicity of crystallizable component in a polymer blend attributable to interlamellar segregation of the second noncrystallizable component has been observed for poly(ϵ-caprolactone)(PCL)/poly(styrene-*co*-acrylonitrile)(SAN),[57] PCL/poly(vinyl chloride) (PVC),[58] and poly(ethylene oxide)/poly(methyl methacrylate) (PEO/PMMA) blends.[59] This suggests that during crystallization of PHB from the one-phase melt, the amorphous P(VAc-*co*-VA) is being rejected into the interlamellar region of PHB, where it forms a homogeneous mixture with the amorphous part of PHB molecules. It has been shown in the literatures that the nature of the segregation process (interlamellar, interfibrillar, or interspherulitic)[55,60] in a miscible blend of a crystallizable polymer with an amorphous one depends on the type of the amorphous polymer.

Generally, the average thickness of the crystalline phase can be estimated by multiplying the long period and crystallinity[57] or one-dimensional correlation function.[61−64] Here, because the spherulite of PHB in the blends 80/20 and 60/40, which crystallized at 95 °C, is space-filling under the polarized optical microscopy, we approximately calculated the average thickness of the crystalline (⟨C⟩n) and amorphous (⟨A⟩n) phases by using the crystallinity data obtained by WAXD and the long period (Figure 13). In Figure 15 the long period, ⟨C⟩n, and ⟨A⟩n of PHB/P(VAc-*co*-VA9) blends are shown. It is seen that the thickness of the crystalline phase decreases from 5.26 to 4.05 nm with addition of the amorphous P(VAc-*co*-VA9).

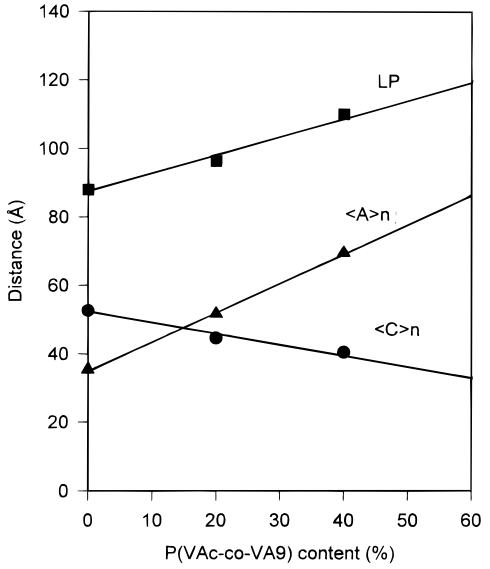

Figure 15. SAXS data of PHB/P(VAc-*co*-VA9) as a function of amorphous P(VAc-*co*-VA9): (■) long period (LP), (●) thickness of the crystalline phase ⟨C⟩n, (▲) thickness of amorphous phase ⟨A⟩n.

Conclusion

Poly(vinyl acetate-*co*-vinyl alcohol) copolymers (P(VAc-*co*-VA)) were synthesized by hydrolysis−alcoholysis of PVAc. The miscibility, crystallization, and morphology of poly(*β*-hydroxybutyrate) (PHB) and P(VAc-*co*-VA) blends were studied by differential scanning calorimetry, optical microscopy, WAXD, and SAXS. It was found that the P(VAc-*co*-VA) (vinyl alcohol content of 9, 15, 22 mol %) can form a miscible phase with the amorphous part of PHB in the solution cast samples. The melting-quenched samples of PHB/P(VAc-*co*-VA) blends with different vinyl alcohol content show different phase behavior. The PHB and P(VAc-*co*-VA9) with low vinyl alcohol content (9%) can form a miscible blend in the melt state. The PHB and the P(VAc-*co*-VA15) with 15% vinyl alcohol cannot form miscible blends, while PHB/P(VAc-*co*-VA15) blend with composition of 20/80 can form a partially miscible blend in the melt state. However, PHB and P(VAc-*co*-VA22) with 22 mol % vinyl alcohol form immiscible blends in the whole composition range. The single glass transition temperatures of the blends within the whole composition range suggest that PHB and P(VAc-*co*-VA9) are totally miscible in the melt. The crystallization kinetics was studied from the whole crystallization process and spherulite growth for the miscible blends. The equilibrium melting point of PHB in the PHB/P(VAc-*co*-VA9) blends, which was obtained from DSC results using the Hoffman−Weeks equation, decreases with the increase in P(VAc-*co*-VA9) content. The negative value of the interaction parameter determined from the equilibrium melting point depression supports the miscibility between the components. The component P(VAc-*co*-VA9) affects the rate of crystallization of PHB in the blends and reduces the rate of crystallization of PHB. The kinetics of spherulitic crystallization of PHB was analyzed according to nucleation theory in the temperature range studied in this work. The best fit of the data to the kinetic theory is obtained by employing WLF parameters and the equilibrium melting points obtained by DSC. The addition of P(VAc-*co*-VA) did not affect the crystalline structure of PHB, as shown by the WAXD results. The long periods of blends obtained by SAXS increase with the increase in P(VAc-*co*-VA) content. It indicates that the amorphous of P(VAc-*co*-VA) was rejected to the interlamellar phase corporating with the amorphous part of PHB.

Acknowledgment. The authors are grateful to the financial supports granted by The National Key Projects for Fundamental Research "Macromolecular Condensed State", The State Science and Technology Commission of China.

References and Notes

(1) Doi, Y. *Microbial Polyesters*; VCH: New York, 1990.
(2) Dawes, E. A. *Microbial Energetics*; Blackie: Glasgow, U. K., 1986.
(3) Holmes, P. A.; Wright, L. F.; Collins, S. H. Eur. Pat. Appl. 0052459, 1981.
(4) Doi, Y.; Kunnioka, M.; Nakamura, Y.; Soga, K. *Macromolecules* **1987**, *20*, 2988.
(5) Doi, Y.; Segawa, Y.; Kunika, M. *Int. J. Biol. Macromol.* **1990**, *12*, 106.
(6) Nakamura, K.; Yoshie, N.; Sakurai, m.; Inoue, Y. *Polymer* **1994**, *35*, 193.
(7) Nakamara, S.; Kunnioka, M.; Doi, Y. *Makromol. Rep.* 1991, A28, 15.
(8) Avella, M.; Martuscelli, E. *Polymer* **1988**, *29*, 1731.
(9) Avella, M.; Greco, P.; Martuscelli, E. *Polymer* **1991**, *32*, 1647.
(10) Pearce, R.; Marchessault, R. H. *Polymer* **1994**, *35*, 3990.
(11) Abe, H.; Doi, Y.; Satkowski, M. M.; Noda, I. *Macromolecules* **1994**, *27*, 50.
(12) Paglia, E. D.; Beltrame, P. L.; Canetti, M.; Seves, A.; Marcandalli, B.; Martuscelli, E. *Polymer* **1993**, *34*, 996.
(13) Marand, H.; Collins, M. *Polym. Prep. Am. Chem. Soc.* **1990**, *31*, 552.
(14) Iriondo, P.; Iruin, J. J.; Fernandez-Berridi, M. J. *Polymer* **1995**, *36*, 3235.
(15) Xing, P.; Dong, L.; An, Y.; Feng, Z. Avella, M.; Martuscelli, E. *Macromolecules* **1997**, *30*, 2726.
(16) Xing, P.; Dong, L.; Feng, H.; An, Y.; Zhuang, Y.; Feng, Z. *Chem. J. Chinese Univ.* **1996**, *11*, 1813.
(17) Greco, P.; Martuscelli, E. *Polymer* **1989**, *30*, 1475.
(18) An, Y.; Dong, L.; Xing, P.; Mo, Z.; Zhuang, Y.; Feng, Z. *Eur. Polym. J.* **1997**, *33*, 1449.
(19) Noyo, K. In *Poly(vinyl alcohol)—properties and applications*; Finch, Ed.; Wiley: New York, 1973; Chapter 4.
(20) Cesteros, L. C.; Isasi, J. R.; Katime, I. *J. Polym. Sci. Polym. Phys.* **1994**, *32*, 223.
(21) Isasi, J. R.; Cesteros, L. C.; Katime, I. *Macromolecules* **1994**, *27*, 2200.
(22) Olibisi, O.; Roberson, L. M.; Shaw, M. T. *Polymer−Polymer Miscibility*, Academic Press: San Diego, 1979.
(23) Azuma, Y.; Yoshia, N.; Sakurai, M.; Inoue, Y.; Chujo, R.; *Polymer* **1992**, *33*, 4763.
(24) Paglia, E. D.; Beltrame, P. L.; Canetti, M.; Seves, A.; Marcandalli, B.; Martuscelli, E. *Polymer* **1993**, *34*, 996.
(25) Pearce, R.; Brown, G. R.; Marchessault, R. H. *Polymer* **1994**, *35*, 3984.
(26) Fox, T. G. *Bull. Am. Phys. Soc.* **1956**, *1*, 123.
(27) Gordon, M.; Taylor, J. S. *J. Appl. Chem.* **1952**, *2*, 493.
(28) Couchman, P. R.; Karasz, F. E. *Macromolecules* **1978**, *11*, 117.
(29) Kwei, T. K.; *J. Polym. Sci., Polym. Lett. Ed.* **1984**, *22*, 307.
(30) Nishi, T.; Wang, T. T. *Macromolecules* **1975**, *8*, 915.
(31) Flory, P. J. *Principles of Polymer Chemistry*; Cornell University Press: Ithaca, 1953.
(32) Hoffman, J. D.; Weeks, J. J. *J. Res. Natl. Bur. Stand.* **1962**, *66*, 13.
(33) Barham, P. J.; Keller, A.; Otun, E. L.; Holmes, P. A. *J. Mater. Sci.* **1984**, *19*, 2781.
(34) Van Krevelen, D. W. *Properties of Polymers*; Elsevier: Amsterdam, 1972.
(35) Imken, R. L.; Paul, D. R.; Barlow, J. W. *Polym. Eng. Sci.* **1976**, *16*, 593.
(36) Paul, D. R.; Barlow, J. W.; Bernstein, R. E.; Wahrmund, D. S. *Polym. Eng. Sci.* **1978**, *18*, 1225.
(37) Ziska, J. J.; Barlow, J. W.; Paul, D. R. *Polymer* **1981**, *22*, 918.
(38) Keith, H. D.; Padden, F. J. *J. Appl. Phys.* **1964**, *35*, 1270.
(39) Cheng, S. Z.; Chen., J.; Janimak, J. J. *Polymer* **1990**, *31*, 1018.
(40) Lovinger, A. J.; Davis, D. D.; Padden, F. J. *Polymer* **1985**, *26*, 1595.

(41) Hoffman, J. D.; Frolen, L. J.; Ross, G. S.; Lauritzen, J. I., Jr. *J. Res. Natl. Bur. Std* 1975, 79A, 671.
(42) Hoffman, J. D.; Davis, G. T.; Lauritzen, J. I., Jr. In *Treatise on Solid State Chemistry*; Hannay, N. B., Ed.; Plenum Press: New York, 1976; Vol. 3, Chapter 7.
(43) Hoffman, J. D. *Polymer* **1983**, *24*, 3.
(44) Runt, J.; Miely, D. M.; Zhang, X.; Galiagher, K. P.; McFeaters, K.; Fishbarn, J. *Macromolecules* **1992**, *25*, 1929.
(45) Saito, H.; Okasa, T.; Hamane, T.; Inoue, T. *Macromolecules* **1991**, *24*, 4446.
(46) Huang, J.; Prasad, A.; Marand, H. *Polymer* **1994**, *35*, 1896.
(47) Williams, M. L.; Landel, R. F.; Ferry, J. D. *J. Am. Chem. Soc.* **1955**, *77*, 3701.
(48) Lauritzen, J.; Hoffman, J. D. *J. Appl. Phys*. **1973**, *44*, 4340.
(49) Roitman, D. B.; Marand, H.; Miller, R. L.; Hoffman, J. D. *J. Phys. Chem*. **1989**, *93*, 6929.
(50) Pearce, R.; Brown, G. R.; Marchessault, H. *Polymer* **1984**, *35*, 3984.
(51) Hoffman, J. D.; Miller, R. L. *Macromolecules* **1988**, *21*, 3038.
(52) Philips, P. J. Rensch, G. J.; Taylor, K. D. *J. Polym. Sci., Polym. Phys. Ed*. **1987**, *25*, 27.
(53) Hoffman, J. D.; Miller, R. L.; Marand, H.; Roitman, D. B. *Macromolecules* **1992**, *25*, 2221.
(54) Canetti, M.; Sadocco, P.; Siciliano, A.; Seves, A. *Polymer* **1994**, *35*, 2884.
(55) Sadocco, P.; Canetti, M.; Seves, A.; Martucelli, M. *Polymer* **1993**, *34*, 3368.
(56) Vonk, C. G. *J. Appl. Cryst*. **1973**, *8*, 81.
(57) Oudhuis, A. A.; Thiewes, H. J.; van Hutten, P. F.; ten Brinke, G. *Polymer* **1994**, *35*, 3926.
(58) Khambatta, F. B.; Warner, F.; Russel, T. P.; Stein, R. S. *J. Polym. Sci., Polym. Phys. Ed*. **1976**, *14*, 1391.
(59) Russel, T. P.; Ito, H.; Wignall, G. *Macromolecules* **1989**, *22*, 1054.
(60) Hsiao, B. S.; Sauer, B. B. *J. Polym. Sci., Polym. Phys. Ed*. **1993**, *31*, 901.
(61) Strobl, G. R.; Schneider, M.; Voigt-Martin, I. *J. Polym. Sci., Polym. Phys. Ed*. **1980**, *18*, 1361.
(62) Talibuddin, S.; Wu, L.; Runt, J.; Lin, J. S. *Macromolecules* **1996**, *29*, 7527.
(63) Verma, R.; Marand, H.; Hsiao, B. S. *Macromolecules* **1996**, *29*, 7767.
(64) Liu, L.-Z.; Chu, B.; Penning, J. P.; Manley, R. St., Jr. *Macromolecules* **1997**, *30*, 4398.

MA980256D